J. Electrochem. Sci. Eng. **15(4)** (2025) 2751; http://dx.doi.org/10.5599/jese.2751

Open Access : : ISSN 1847-9286
www.jESE-online.org

Original scientific paper

Development of graphite-epoxy screen-printed electrodes selective to nitrate ions

Leodanis Correa Fajardo[1], Abel Ibrahim Balbín Tamayo[1,✉], Yusleydi Enamorado Horrutiner[1], Ana Rosa Lazo Fraga[2] and Ana Margarita Estevas Guas[1]

[1]*Department of Analytical Chemistry, Faculty of Chemistry, University of Havana, Havana, Cuba*
[2]*Institute of Materials Science and Technology, University of Havana, Havana, Cuba*

Corresponding author: ✉*ibrahimaries009@gmail.com*

Received: April 9, 2025; Accepted: May 19, 2025; Published: June 16, 2025

Abstract

High concentrations of nitrate ions in water can cause eutrophication, while ingestion of these ions can cause methemoglobin and various cancers. Therefore, there is a need for sensitive, selective and inexpensive analytical tools, as an alternative to expensive conventional techniques, to monitor and evaluate the concentration of these ions. The aim of the present investigation is to develop printed graphite-epoxy electrodes modified with PVC membranes for the potentiometric determination of nitrate ions. The electrodes were manually printed in the laboratory with inks prepared from epoxy resin and graphite at different percentages and particle sizes. The printed electrodes were characterized by cyclic voltammetry, electrochemical impedance spectroscopy and scanning electron microscopy, prior to their modification with PVC membrane. The chrono-potentiometric response of the electrodes was evaluated with NO_3^- ion solutions. The best printing and electrochemical behavior of electrodes was obtained with inks containing 76 % of modified conductive phase-modified graphite nanoparticles. The developed ion-selective electrodes showed response to nitrate ions with a super-Nernstian slope, detection limits in the order of 10 μmol L^{-1}, response times of 10 to 12 seconds and selectivity in the presence of NO_2^-, SO_4^{2-}, Cl^-, Br^-, I^- and CrO_4^{2-} ions. The developed electrodes were used for the indirect determination of chloride ions in water samples by potentiometric titration.

Keywords

Electrochemical nitrate sensor; ion-selective electrode; selective membrane; cyclic voltammetry; potentiometry

Introduction

Water pollution is an environmental problem that represents one of the most pressing challenges facing society today. Presence of nitrate ions in water bodies has emerged as a major concern due to its significant impact on water quality and, consequently, on human health [1]. The World Health Organization (WHO) and Australian regulations have set a guideline value of 50 mg L^{-1}, while the

United States Environmental Protection Agency (EPA) has set a maximum contaminant level (MCL) for nitrate in drinking water of 44.2 or 10 mg L^{-1} (as total nitrogen) [2,3].

Nitrate ions are very common contaminants in drinking water. They are mainly caused by the excessive use of nitrogen fertilizers in agriculture and the lack of management of animal excreta generated in livestock farming. In nature, this ion is naturally present, but any anthropogenic alteration of the natural nitrogen cycle modifies the permissible levels of this pollutant in water [4,5]

Given the risks that nitrate ions pose to the organism, the determination of these contaminants in water at trace levels is of great importance. A variety of analytical techniques have been reported in the literature for the determination of this ion, including spectrophotometry, chromatography, spectrofluorimetry, and others [6-8]. In addition to these expensive and complex automated instruments for nitrate analysis, chemical sensors have been developed. These devices are alternative analytical techniques due to their simplicity, robustness, portability and low cost.

Among the chemical sensors, electrochemical sensors for the determination of nitrate ions, especially the all-solid-state electrodes, stand out in the literature. Despite a large number of publications on nitrate ion-selective electrodes, research continues to focus on the development of new electrodes that are more robust, economical, portable, require small sample volumes for analysis, can be produced in large quantities, and can be integrated into portable devices for *in situ* measurements. Table 1 summarizes the characteristics of various already reported potentiometric sensors.

Table 1. *Characteristics of some sensors for potentiometric nitrate detection, Ag/AgCl reference electrode*

Material	Nernstian slope, mV dec^{-1}	LOD, mol L^{-1}	Detection range, mol L^{-1}	Ref.
CS-MMT nanocomposite and graphite-epoxy	-49 to -54	7×10^{-5}	10^{-5} to 0.1	[9]
Zn(II) complexes coordinated by neutral tetradentate ligands on PVC	-55.16	1.86×10^{-5}	10^{-5} to 0.1	[10]
Polypyrrole nitrate and tridodecylmethylammonium nitrate modified graphite electrode immobilized on PVC	-53.99	8×10^{-4}	10^{-5} to 1.0	[11]
Epoxy-graphite composite and PVC membrane	-59.5	1.5×10^{-4}	1.6×10^{-4} to 0.016	[12]
Glassy carbon electrode and polypyrrole with nitrate doped	-55.0	10.0^{-4} to 0.8	Not reported (>8×10^{-6})	[13]
Chitosan/bentonite nanocomposite modified graphite-epoxy electrode	-54.6	2×10^{-4}	2×10^{-4} to 0.8	[14]

In recent years, screen printing has been used to fabricate printed electrodes. The most important feature of these electrodes is the construction of a new generation of miniaturized sensors that can meet the requirements of portable analytical devices and can replace conventional electrodes [15]. Some reports have been made by Koncki *et al*. [16], Jiang *et al*. [17], Baumbauer *et al*. [18], Thuy *et al*. [19] and Paré *et al*. [20].

Publications on solid-state printed electrodes for the potentiometric determination of nitrate ions are still lacking. Therefore, the main objective of this work is to develop a miniaturized graphite-epoxy electrode selective for nitrate ions by modifying screen-printed electrodes with PVC sensing membranes.

Experimental

Reagents

All reagents used were of analytical grade (>99 %). Deionized water with a conductivity of 1.26 µS cm^{-1} was used. Mixtures of Merk's 50 µm powdered graphite and epoxy resin were prepared for the construction of the electrodes as previously reported [21]. The nanometric graphite used as an ink modifier (a mixture of multi-walled carbon nanotubes, carbon nanobeads, amorphous graphite, micrometric graphite, graphite oxide and carbon quantum dots) was synthesized by the submerged arc discharge method at the Center for Technological Applications and Nuclear Development (CEADEN) [22-25]. The redox couple $[Fe(CN)_6]^{3-/4-}$ with a concentration of 0.02 mol L^{-1} was prepared using potassium hexacyanoferrate(II) trihydrate and potassium hexacyanoferrate(III) (Merk, Germany) in equimolar amounts in 0.02 mol L^{-1} phosphate buffer saline solution (PBS) buffer pH 6.9 from Sigma Aldrich. The membrane was prepared using PVC from UNI-CHEM, tributyl phosphate and tetrahydrofuran from ALDRICH, and 1-furoyl-3,3-diethylthiurea as ionophore, synthesized by the Laboratory of Organic Synthesis, Faculty of Chemistry, University of Havana [26,27]. KNO_3 from ALDRICH and $Pb(NO_3)_2$ from FLUKA were used to evaluate the potentiometric response of the electrodes. For the interference study, K_2CrO_4 from MERCK, KBr from AnalaR, KI from FLUKA, KCl from PANREAC, Na_2SO_4 and $NaNO_2$ from UNI-CHEM were used. Pure NaOH (> 99 %) and HNO_3 from MERCK were used for the pH study.

Equipment

Electrodes were cured in a DHG-9146A oven (China). Electrical resistance measurements were performed with a YFE model YF-2100 digital multimeter. Electrochemical characterization and potentiometric evaluation were performed using a Palm Sens 4 potentiostat (Italy) connected to a computer managed by PSTrace software version 5.9 and operating in cyclic voltammetry (CV), electrochemical impedance spectroscopy (EIS) and open-circuit potential (OCP) modes. A three-electrode system, a graphite-epoxy screen-printed working electrode, a platinum auxiliary electrode and the Ag/AgCl reference electrode (KCl, 3 mol L^{-1}) from Basic Analytical Systems (BAS) was used. Deionized water was obtained from the water purifier, Milli-Q, HPW Pure Water System, Heal-Force (China). The pH study was carried out using a pH meter, model PHSJ-3F (China) and a glass membrane electrode from HANNA Instrument. Microscopy was performed in a scanning electron microscope (SEM), model Vega 5130 SB, TESCAN, with a tungsten filament electron source (OXFORD Instruments).

Preparation of graphite-epoxy inks and electrode screen printing process

Six composite mixtures were prepared according to previously reported results [21]. 1-butanol and benzyl alcohol were used in different volume ratios until the appropriate viscosity for printing was achieved. Table 2 shows the content of graphite with respect to the total mass of the composite (insulating phase-epoxy resin + conductive phase-graphite) and the volume ratio between the solvents used.

Table 2. *Composition of graphite-epoxy inks*

Ink/printing	Content of graphite (50 µm), %	1-butanol : benzyl alcohol volume ratio
A	50.8	6 : 1
B	61.4	25 : 1
C	76.0	50 : 1
C-1	76.0	1 : 3
C-2	76.0	1 : 4
C-3	68.4 (+ 7.6 nanometer graphite)	1 : 4

The electrodes were printed on polyethylene terephthalate (PET) sheets using a screen-printing frame with the electrode template and a pore size of 100 μm. The screen-printed electrodes were then dried in an oven at 40 °C for 48 h to achieve curing of the electrodes [21,28], and the working area and the electronic contact area were then isolated with insulating tape.

Preparation of PVC membranes and construction of nitrate ion selective screen-printed electrodes

Membranes were prepared by mixing 62% tributyl phosphate, 28 % PVC and 10 % 1-furoyl-3,3--diethylthiurea (ionophore) with 600 μL of tetrahydrofuran [29]. In addition, membranes without the ionophore (blank membranes) were prepared with equal amounts of the remaining components. The PVC membranes were manually applied to the screen-printed electrodes, which showed a potential difference of 1.4 mV in front of the redox system $[Fe(CN)_6]^{3-/4-}$. Ion-selective electrodes (ISEs) were dried for 24 h and then activated in a solution of 10 mmol L^{-1} NO_3^- ions for 24 h.

Experimental procedures

Electrochemical characterization was performed by cyclic voltammetry (CV) and electrochemical impedance spectroscopy (EIS) techniques. A three-electrode system was used to evaluate the electrochemical response of the screen-printed electrode to the redox system $[Fe(CN)_6]^{3-/4-}$. Cyclic voltammograms were obtained at the interval -2.0 and 2.0 V, at 25 mV s^{-1}. Electrochemical impedance spectra were measured at the open circuit potential (OCP), in a frequency range between 100 kHz to 0.05 Hz with an alternating signal amplitude of 10 mV.

To evaluate the repeatability of the screen-printing process, three replicates of the carbon ink were printed, corresponding to the electrodes that showed the best electrochemical behavior in the redox system $[Fe(CN)_6]^{3-/4-}$. A random selection of 45 electrodes was made in each case, the electrical resistance was measured with a digital multimeter and a hypothesis test for the comparison of the three-sample means was performed by analysis of variance (ANOVA) using STATGRAPHICS 19 software (free version) [30].

The potentiometric response of the sensors was evaluated using the addition method described by IUPAC [31]. Starting from a three-electrode system, aliquots of $Pb(NO_3)_2$ were added every 1 min to the electrochemical cell with 10 mL of deionized water, and the variation of the equilibrium potential over time was measured. The activation process was evaluated in water and in $Pb(NO_3)_2$ and KNO_3 solutions. Electrode calibration was performed with KNO_3 (the concentration was varied from 2×10^{-6} to 22 mmol L^{-1}) solutions for electrodes activated in $Pb(NO_3)_2$.

SEM characterization was performed on the working area of the printed electrode coated with gold vapor. An electron beam accelerated to a potential of 15 kV was used to obtain the micrographs at different magnifications.

The response time of the sensors was evaluated at OCP by adding successive aliquots of 50 μL KNO_3 at 1 mol L^{-1} to a solution of KNO_3 at 1 mmol L^{-1}. The stability criterion was taken as a change in potential equal to, or less than 1 mV min^{-1} [32].

To evaluate the influence of pH on the electrode potential, the potential was stabilized in 25 mL of 10 mmol L^{-1} HNO_3, successive additions of NaOH at 0.1 and 1 mol L^{-1} were made, and pH of the solution and electrode potential values were measured simultaneously after each addition.

The interference study was performed according to the mixed-solution method [33]. This method consisted of performing calibrations with KNO_3 (concentration range 2×10^{-6} to 22 mmol L^{-1}) and 10 mL of the interfering ion at 1 mmol L^{-1}. The influence of the ionic species NO_2^-, SO_4^{2-}, CrO_4^{2-}, Cl^-, Br^- and I^- was evaluated by determining the potentiometric selectivity coefficient.

In order to determine the lifetime of the developed sensors, the variation of sensitivity of electrodes over time was evaluated, which consisted of performing triplicate calibrations for unmodified electrodes and those modified with PVC membranes at 2, 11, 30 and 120 days after activation with $Pb(NO_3)_2$.

The developed ISEs were used for the indirect determination of chloride ions in synthetic samples by potentiometric titration with $AgNO_3$. Titration curves were obtained at two chloride ion concentration levels (10 and 50 mmol L^{-1}). From the concentration data estimated by ISE, a three-factor nested design (factor 1: electrode, factor 2: operator and factor 3: replicates) was performed, which allowed the precision to be estimated under repeatability conditions and under intermediate precision conditions between operators, between electrodes and between operators and electrodes.

Results and discussion

Electrochemical characterization by cyclic voltammetry

Figure 1a shows the cyclic voltammograms obtained for the electrodes of print A, B and C against the redox system $[Fe(CN)_6]^{3-/4-}$. No electrochemical signals corresponding to the oxidation-reduction processes of the redox system are shown for the electrodes of prints A and B. This behavior may indicate a high resistance to electron transfer, which justifies an insulating behavior. For the electrodes corresponding to print C (76 %), electrochemical signals corresponding to the oxidation-reduction processes of the redox probe were observed. In this case, the cyclic voltammograms showed two separate peaks at a potential difference of 3.3 ± 0.2 V.

From the previous results, it was found that 76 % of the conductive phase was sufficient to generate electrochemical response of the electrodes, so two prints (print C-1 and C-2) were made with the same composition of ink C, varying the volume ratio between the solvents in searching better print of the electrode (Table 2). In addition, a print C-3 was made by modifying the conductive phase with nanometric graphite to improve the percolation threshold of the conductive charge. Figure 1b shows the cyclo-voltammograms obtained for these electrodes, where a better electrochemical behavior is observed for the electrodes of print C-2 with respect to those of print C-1, indicating an improvement in the screen-printing process with the proportions of solvents used. The electrochemical signal was improved further when nanometric graphite was incorporated into the carbon inks (print C-3).

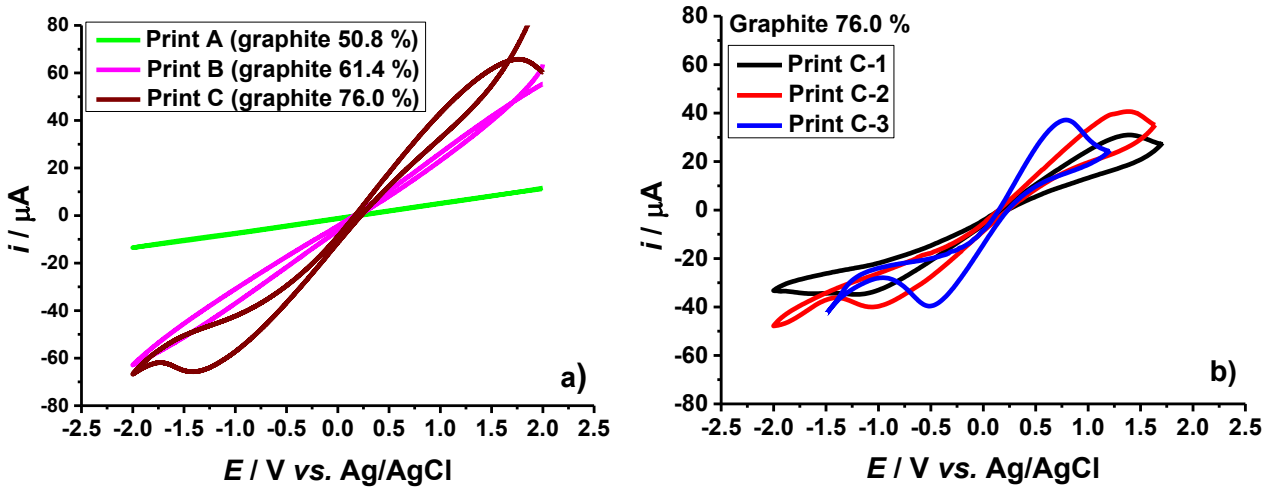

Figure 1. *CVs of denoted graphite-epoxy screen-printed electrodes for 0.02 mol L^{-1} $[Fe(CN)_6]^{3-/4-}$ in 0.02 mol L^{-1} PBS pH 6.9, at a scan rate of 25 mV s^{-1}*

The CVs obtained for the C-3 print showed defined signals and high symmetry, with the potential difference between the peaks decreasing to 1.4 ± 0.1 V and the cathodic and anodic peak current intensities increasing significantly compared to the other prints.

These results are due to the fact that the smaller size of the graphite nanoparticles increases the probability of occupancy in the conductive network in the insulating matrix, the critical probability or percolation threshold of the conductive charge and the electroactive area on the surface of the printed electrodes, which is reflected in an improvement of the conductivity of the charge carriers. A larger electroactive surface area influences the charge transfer and the electron transfer rate during redox processes. The smaller power difference observed compared to the other printed electrodes indicates that the oxidation-reduction processes on the electrode surface occur at a lower overpotential and lower energy cost. According to Nicholson *et al*. [34], a smaller potential difference between the peaks in the cyclic voltammograms indicates a higher value of the heterogeneous electron transfer constant (k^o) and thus faster electron transfer kinetics.

Electrochemical characterization by EIS

The electrodes corresponding to each print were characterized by EIS in order to analyse the behavior of the electron transfer resistance with respect to the percentage of micrometric graphite and the use of nanometric graphite in the carbon inks. Figure 2 shows the Nyquist plots for each electrode analysed, along with the equivalent circuits used to model the electrode impedance spectra.

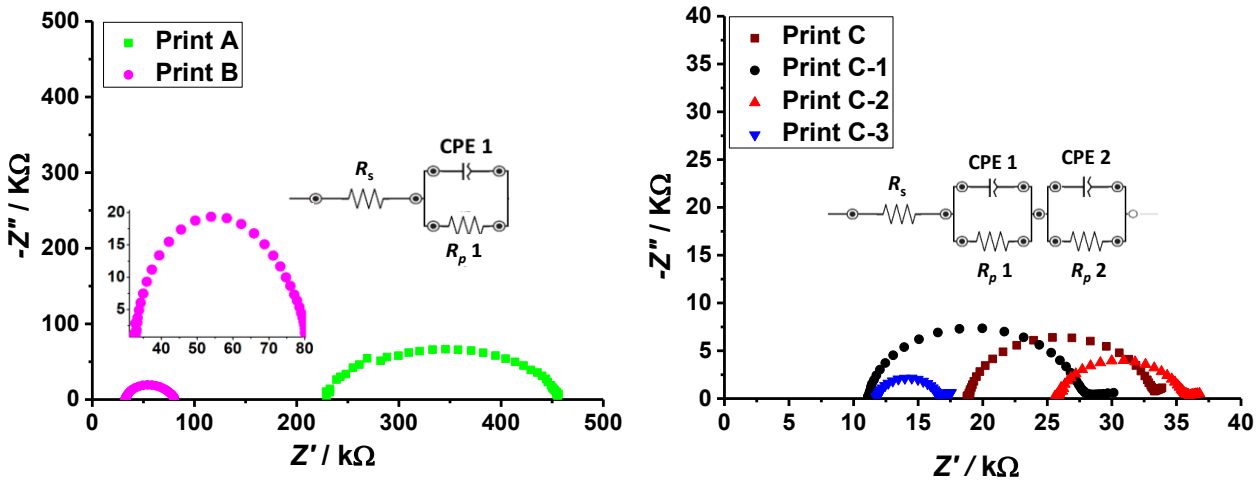

Figure 2. *Nyquist plots of the screen-printed electrodes of each print, measured over a frequency range of 10^5Hz - 0.05 Hz, at OCP. Electrolyte solution: 0.02 mol L^{-1} of $[Fe(CN)_6]^{3-/4-}$ in 0.02 mol L^{-1} PBS pH 6.9*

The difference in the impedance results obtained for the electrodes of prints A and B with respect to the other prints is due to the fact that the former two have a high resistance to electron transfer.

The impedance response obtained in all cases was interpreted by establishing an analogy between the physicochemical processes occurring at the electrode material and the impedance response of equivalent circuits. In the proposed equivalent circuits, R_s represents the resistance associated with the contacts, cables, connections, *etc*, while R_p 1 is the resistance associated with the transducer or printed electrode. The circuit elements CPE 2 and R_p 2 correspond to the mechanisms associated with the electrode-solution interface observed at low frequencies for the C, C-1, C-2 and C-3 prints. It should be emphasized that in the Nyquist impedance spectra the maximum value of the imaginary impedance component (-*Z*'') is lower than the semicircle radius (R_p/2) for all the electrodes analysed, which justifies the use of a constant phase element (CPE) instead of a capacitor in the proposed equivalent circuits, in order to obtain a better fit between the experimental and modeled data.

The fit between the experimental impedance data and the impedance response modeled with the electrical circuits yielded Chi-squared values (χ^2) between 10^{-4} and 10^{-5}, indicating a reasonable fit. From the R_p 1 values, it was found that the electrode resistance decreases from print A to print C, which is consistent with the increase in the percentage of graphite in the material. The lowest resistance values were obtained for electrodes corresponding to print C-3, which corresponds to electrodes containing nanometer graphite. These results are consistent with the properties of the electrodes with the increase in the percentage of graphite and the use of nanometric graphite.

Evaluation of the repeatability of the C-3 ink printing process

The repeatability of the screen-printing process of the ink corresponding to this C-3 printing was evaluated. The inks were prepared in triplicate (print C-3a, print C-3b, print C-3c), 45 electrodes were selected from each print, the electrical resistance was measured, and an analysis of variance (ANOVA) was performed to compare the sample means.

Table 3 shows the results of the normality test using the χ^2 and Shapiro-Wilks statistical tests, and the homogeneity of variances test using the Bartlett and Cochran tests, performed after eliminating the anomalous resistance values (H_o is the null hypothesis and H_i is the alternative hypothesis). The normality test indicated with 95 % confidence that the resistance values of the three prints performed were from a normal distribution. The analysis of homogeneity of variances showed that the probability values are greater than 0.05, therefore, it can be said with 95 % confidence that the variances are homogeneous. H_o was not rejected in either test.

Table 3. *Probability values for the test of normality and homogeneity of variances, for α = 0.05*

Test of normality			
Hypothesis testing	Print	*P* values	
		χ^2	Shapiro-Wilks
H_o: Print C-3a, C-3b and C-3c come from a normal distribution. H_i: Print C-3a, C-3b and C-3c do not come from a normal distribution	C-3a	0.0515	0.1086
	C-3b	0.0619	0.2936
	C-3c	0.5227	0.5875
Homogeneity of variances test			
Hypothesis testing		*P* values	
		Bartlett	Cochran
H_o: $\sigma_{print\text{-}3a}^2 = \sigma_{print\text{-}3b}^2 = \sigma_{print\text{-}3c}^2$		0.7764	0.9146
H_i: $\sigma_{print\text{-}3a}^2 \neq \sigma_{print\text{-}3b}^2 \neq \sigma_{print\text{-}3c}^2$			

α: probability of committing a Type I error, which is rejecting the null hypothesis when it is actually true, σ^2: dispersion or population variance

The analysis of variance for the comparison of the three-sample means (Table 4) yielded a probability value greater than 0.05, allowing us to say with 95 % confidence that the means are statistically equal.

Table 4. *Results of the analysis of variance (ANOVA) for the values of the resistance of the three inks prepared*

Source	Sum of squares	*df*	Mean square	*F*-ratio	*P*-value
Between groups	13.6778	2	6.83888	1.88	0.1565
Within groups	439.356	121	3.63104		
Corrected total sum of squares	453.033	123			
H_o: $\sigma_E^2 = \sigma_D^2 \rightarrow \mu_{print\text{-}3a} = \mu_{print\text{-}3b} = \mu_{print\text{-}3c}$; H_i: $\sigma_E^2 >> \sigma_D^2 \rightarrow \mu_i \neq \mu_j$					

df: degree of freedom; σ_E^2: dispersion between groups; σ_D^2: Dispersion within groups; μ: population mean

These statistical results allow us to affirm that the printing process of the graphite-epoxy electrodes is reproducible, therefore, it can be considered that all the resistance values of the electrodes belong to the same population, with a confidence interval of 9 ± 2 kΩ.

Potentiometric response of graphite-epoxy screen-printed electrodes modified with PVC membranes

The electrodes corresponding to the C-3 print, whose resistance values, measured with a digital multimeter, were found to be within the confidence interval of 9 ± 2 kΩ, were used for the construction of the ISE by deposition of PVC sensing membranes. Figure 3a shows the potentiometric response obtained for three electrodes using the addition method, where a potentiometric response corresponds to an anionic response behavior (negative response slope). The result obtained is in agreement with that published by Arada-Pérez and collaborators [26], where graphite-epoxy electrodes modified with PVC sensing membranes are reported for the determination of lead(II) and nitrate ions. The response to nitrate ions occurs when the ISE no longer responds to the Pb(II) cation, due to loss by exudation of a component of the membrane or saturation of the active sites in the membrane, *i.e*. free thiourea to coordinate with the metal ion [26].

In order to know the electrode component responsible for the response to nitrate, the potentiometric response of unmodified electrodes, electrodes modified with white PVC membrane and electrodes modified with 10 % PVC membrane of 1-furoyl-3,3-diethylthiurea, to changes in the concentration of $Pb(NO_3)_2$ in the measurement cell was evaluated. Figure 3b shows the potentiometric response obtained in each case, where a potentiometric response to nitrate ions is observed in all cases. These results show that the ionophore is not the cause of the nitrate ion response of the ISE. The potentiometric response is mainly due to the transducer and the dummy PVC membrane components (without the ionophore). Therefore, it was decided to omit the ionophore in the preparation of the membranes and to perform the ISE evaluation with the white PVC membrane only.

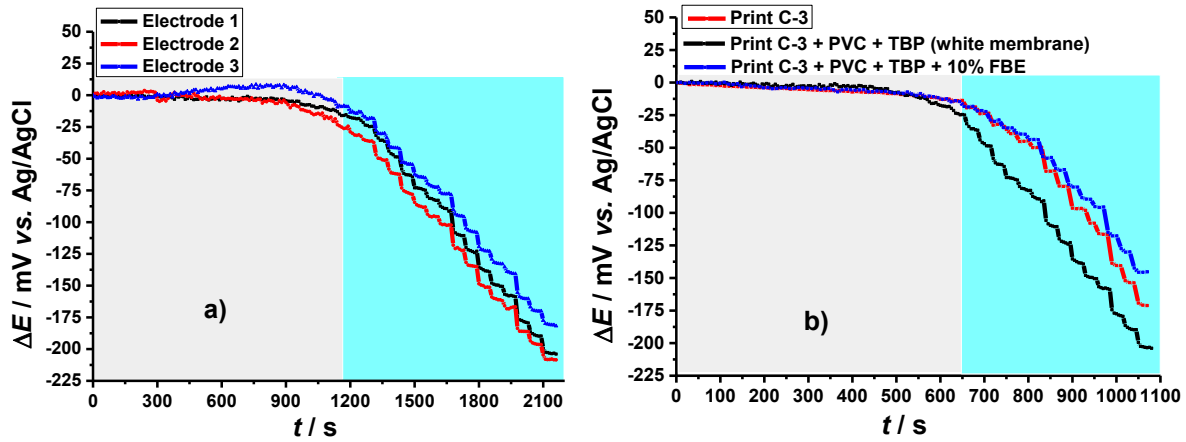

Figure 3. *Chronopotentiometric responses of (a) three printed electrodes (print C-3) modified with 10 % PVC membranes of the ionophore 1-furoyl-3,3-diethylthiurea (FDB), (b) each electrode component (transducer only, transducer + blank membrane and transducer + 10 % FDB membrane)*

The response to nitrate ions corresponding to the unmodified electrode can be explained by the possible presence of amino groups in the transducer, which are formed during the curing process between the epoxy resin and the amine used as a hardener. As reported by Matějka *et al.* [35], during the curing process of an epoxy resin, the presence of tertiary amines could react with the epoxy group to form a zwitterion containing a quaternary nitrogen atom, which in the present investigation could be responsible for the potentiometric response to nitrate ions.

Analysis of the activation process

The activation process of the unmodified and modified electrodes with white PVC membranes was studied in different media (KNO_3, $Pb(NO_3)_2$ and H_2O) to determine the most sensitive conditions

in the developed ISEs. Figure 4 shows the ΔE *vs*. log $a(NO_3^-)$ curves obtained. The results show that the potentiometric response depends on the activation process prior to calibration. From the linear regression parameters (Table 5), it was obtained that activation with $Pb(NO_3)_2$ causes a higher sensitivity to nitrate ions for both types of electrodes.

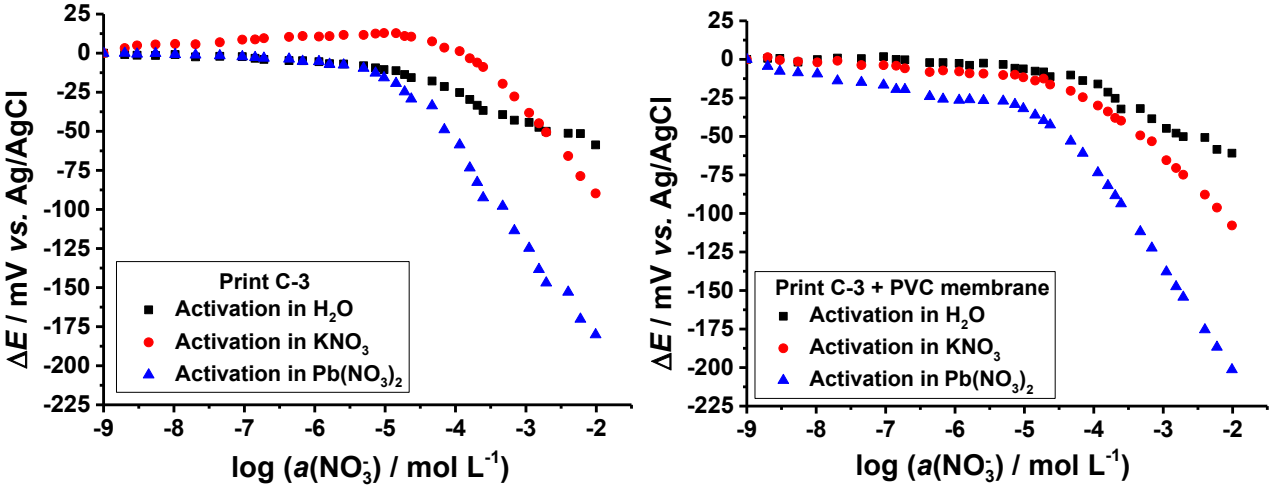

Figure 4. *ΔE vs. log a(NO_3^-) curves for unmodified printed electrodes (print C-3) and printed electrodes modified with PVC membranes (print C-3 + PVC membrane), activated in different media*

Table 5. *Parameters of the linear regression in the Nernstian zone of the* Δ E vs. *log* a*(NO_3^-) curves*

Print C-3			Print C-3 + PVC membrane		
Activation	r^2	S / mV dec^{-1}	Activation	r^2	S / mV dec^{-1}
in H_2O	0.958	-17 ± 1	in H_2O	0.973	-23 ± 1
in KNO_3	0.992	-49 ± 1	in KNO_3	0.986	-38 ± 1
in $Pb(NO_3)_2$	0.988	-62 ± 2	in $Pb(NO_3)_2$	0.998	-65.2 ± 0.7

r^2: correlation coefficient; S: slope response of the electrode in the Nernstian region (sensitivity of the electrode)

The activation process of the unmodified and modified graphite-epoxy electrodes with PVC membranes was additionally studied by scanning electron microscopy to detect possible surface changes of the electrodes after the activation process, which justify the potentiometric response shown in Figure 4. Figure 5 shows the micrographs obtained for the unmodified electrodes, in which no appreciable changes were detected on the surface of the electrodes activated with water and potassium nitrate.

Figure 6 shows the micrographs obtained for the electrodes modified with white PVC membranes. In the membranes activated in water, a high formation of surface craters was observed, in addition to white particles associated with the presence of moisture, since they disappeared when the image was amplified at these points. A similar behavior was observed for membranes activated in potassium nitrate, where white clusters could be associated with potassium nitrate particles.

In membranes activated with $Pb(NO_3)_2$, the white spots could be associated with solid particles of the nitrate salt, results also reported by other authors for PVC membranes activated with $Pb(NO_3)_2$ [29]. It is important to highlight the formation of nanometer-sized dots in these membranes (Figure 6c1, 40000× magnification), which could be associated with the formation of sites that improve the sensitivity of the electrodes, due to the interaction that could exist between the amino groups of the transducer and the lead ions. These interactions could be possible due to the low thickness, porosity and permeability of the membrane.

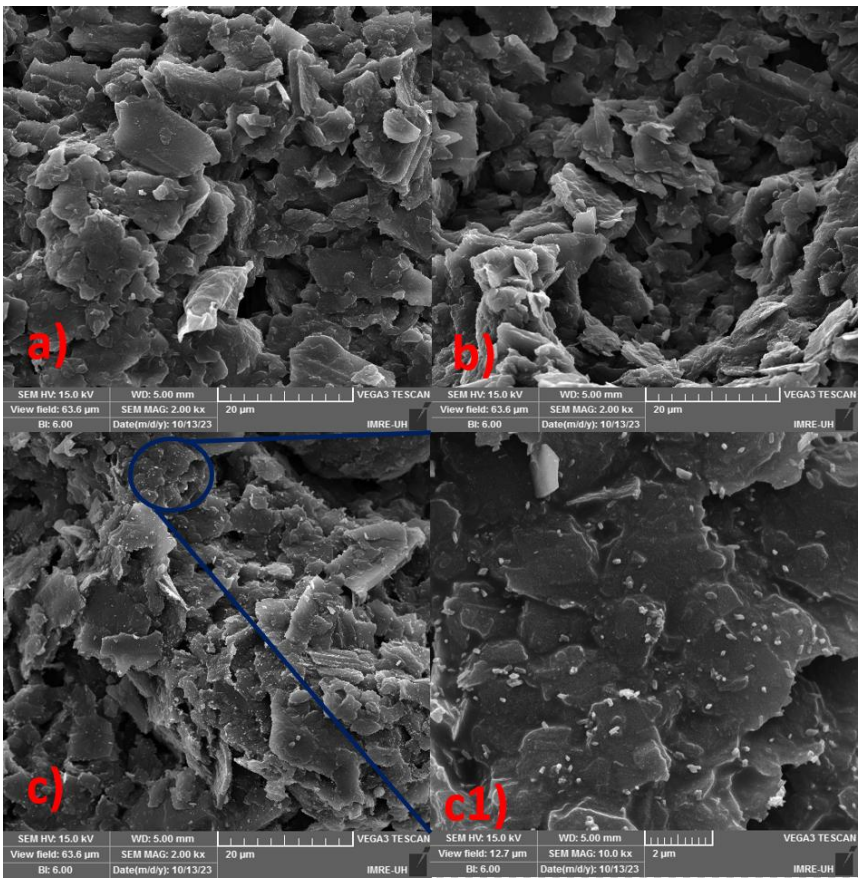

Figure 5. *SEM micrographs corresponding to the unmodified epoxy graphite electrodes: (a) activation in H_2O, (b) activation in KNO_3, (c, c1) activation in $Pb(NO_3)_2$, different magnification*

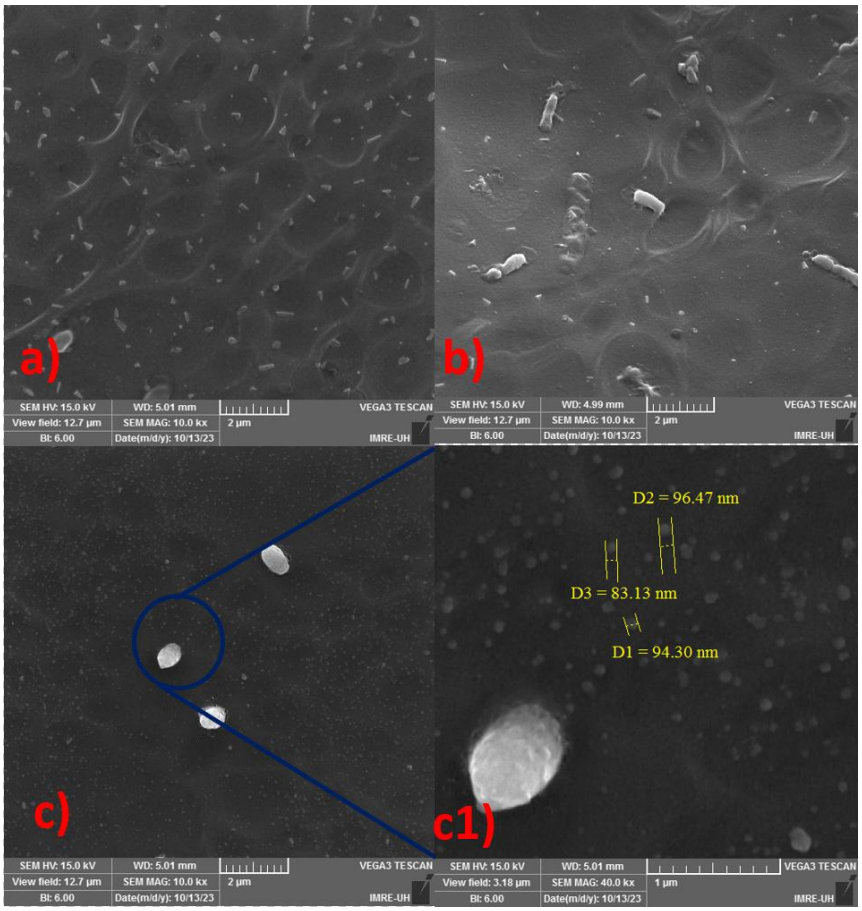

Figure 6. *SEM micrographs corresponding to the epoxy graphite electrodes modified with PVC membranes: (a) activated in H_2O, (b) activated in KNO_3, (c, c1) activated in $Pb(NO_3)_2$ at different magnifications*

Electrode calibration

Figure 7 shows the calibration curves obtained for each replicate analysed, for unmodified electrodes and for electrodes modified with white PVC membranes.

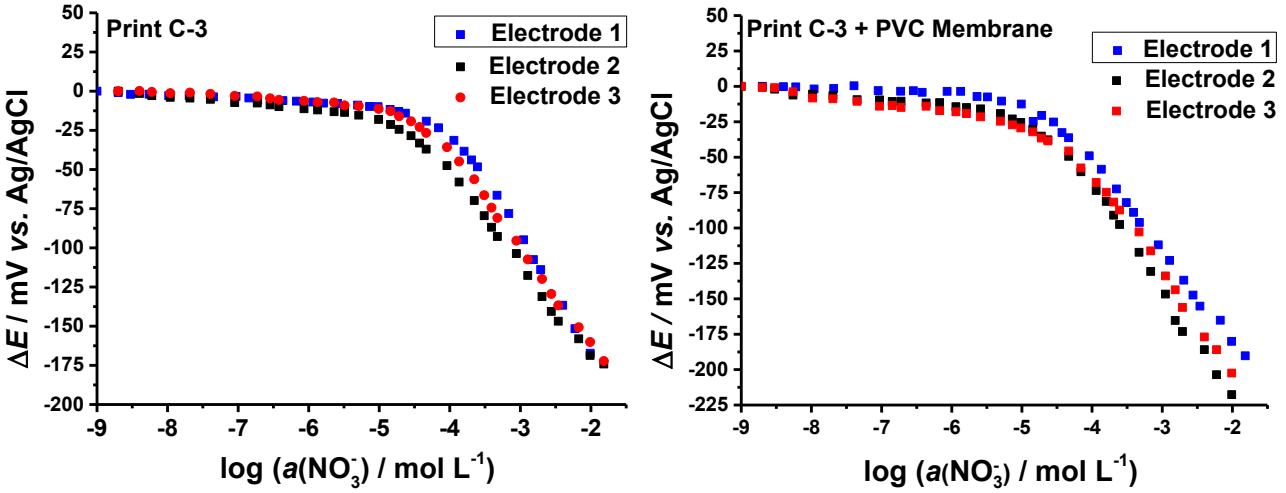

Figure 7. *ΔE vs. log a(NO_3^-) for unmodified printed electrodes (print C-3) and printed electrodes modified with white PVC membranes (print C-3 + PVC membrane)*

The calibration parameters of the developed sensors, such as sensitivity (*S*), lower linear response limit (LIRL) and practical limit of detection (LPD), were determined by linear regression on the calibration curve, in a linearity range in the order of 0.1 to 10 mmol L^{-1}. The results obtained are shown in Table 6**.**

Table 6. *Performance parameters obtained during electrode calibration*

Parameters	Electrodes	
	Print C-3	Print C-3 + PVC membrane
r^2	0.997	0.996
S / mV dec^{-1}	-62.2 ± 0.7	-69 ± 5
LIRL, μmol L^{-1}	47.8 ± 0.8	40.0 ± 10.0
LPD, μmol L^{-1}	37.0 ± 7.0	24.0 ± 6.0
Response time, s	10	12

The linear regression in the Nernstian region of the calibration curves was statistically significant, with a coefficient of determination greater than 0.99 in all cases. The response slope values show that the sensitivity of the electrodes modified with PVC membrane is slightly higher than that of the unmodified electrodes. In both cases, the values are higher than the theoretical value reported by Nernst for a monovalent ion (59.16 mV dec^{-1}) [31], indicating a supernormal behavior, a result in agreement with that reported by some authors using PVC membranes selective for nitrate ions [26,36,37].

The super-Nernstian behavior in some ion-selective electrodes is not known in depth, but some theories are reported that try to explain this phenomenon. Studies by Amemiya *et al.* [38,39] suggest that the super-Nernstian behavior in electrodes is due to the interaction between the receptor element of the electrode and the secondary ions in the membrane phase. This can occur when the secondary ions have an opposite charge to the primary ion (or ion of interest, NO_3^-) and bind independently to the ISE receptor element. This interaction that the secondary ion may experience can enhance the response of the electrode at lower concentrations of the primary ion, resulting in a super-Nernstian response.

Effect of pH on the potentiometric response

Figure 8 shows the Reilley plots obtained when analysing the influence of solution pH on electrode's response. The optimum pH range was found to be between 4 and 10 for both electrodes. For the unmodified electrodes, the potential remains practically constant throughout the pH range studied, since the electrode responds preferentially to the ion of interest and the influence of pH is small. In this case, the variation experienced by the concentration of nitrate ions during the pH analysis is not significant enough to cause an appreciable variation in the potential. On the other hand, in the electrodes modified with white PVC membrane, the potential showed some stability at pH values between 4 and 10. It is important to note that in this pH range, the electrodes show a higher analytical signal compared to the unmodified electrodes.

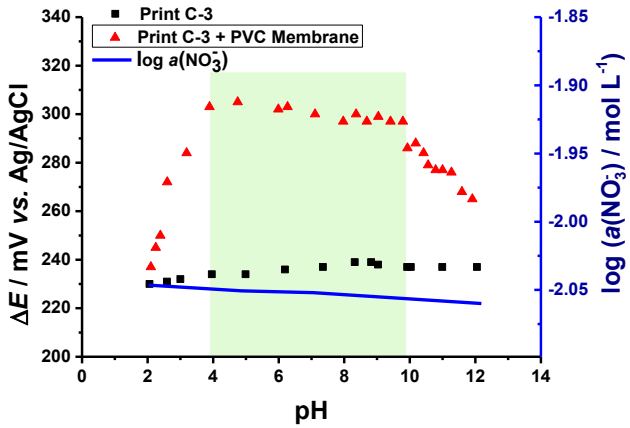

Figure 8. *Variation of ΔE with pH for printed electrodes without membrane and with PVC membranes, (in blue the variation of log a(NO_3^-) vs. pH)*

The differences obtained in the behavior of ΔE *vs.* pH could be mainly due to the PVC that constitutes the membrane of the modified electrodes. Some authors report that the PVC structure is affected at extreme pH values. Under certain conditions, the structure of polyvinyl chloride can be affected at basic pH in the presence of strong bases acting as nucleophiles [40,41]. At acidic pH, PVC degradation can be catalyzed [42]. Possible changes in the PVC structure by varying the pH of the medium can lead to changes in the membrane surface of the electrodes and consequently to changes in the membrane permeability, resulting in variations in the membrane phase potential [42].

Analysis of possible interfering ions

One of the most important parameters to evaluate when studying an ion selective electrode is its selectivity, which is expressed by calculating the potentiometric selectivity coefficient (*K*) (Equation (1)), where: *a* is the activity of the NO_3^- ion and the interfering ion (j), *Z* is the charge of the ion. The determination of this analytical parameter allows the definition of the future applications of the sensor in the analysis of real samples.

$$K_{NO_3^-,j}^{pot} = \frac{a_{NO_3^-}}{a_j^{Z_{NO_3^-}/Z_j}} \quad (1)$$

Table 7 shows the values of the potentiometric selectivity coefficients obtained by the mixed-solution method for NO_2^-, SO_4^{2-}, Br^-, Cl^-, I^-, CrO_4^{2-} ions at a concentration of 10^{-3} mol L^{-1}. These ions are the most frequently reported in the literature for interference studies on nitrate-selective

electrodes [43,44]. In addition, many are controlled by the Cuban standards 827:2017 and 1021:2014 on the quality of water for human consumption [45,46].

The results show that for both types of electrodes (with and without membrane), the potentiometric selectivity coefficient is less than one for all interfering ions. This result indicates that the selectivity of the electrode favors the nitrate ion [47]. The values of the potentiometric selectivity coefficient for the electrodes modified with PVC membranes were slightly lower, indicating a higher selectivity for nitrate ions than for the electrodes without membrane. This could be related to a permeoselective effect of the PVC membrane. In both cases, SO_4^{2-} and CrO_4^{2-} ions are non-interfering ions.

Table 7. *Potentiometric selectivity coefficient of printed electrodes without membrane with white PVC membrane*

Interfering ion	Electrodes	
	Print C-3	Print C-3 + PVC membrane
	K^{pot}	
NO_2^-	0.285	0.248
SO_4^{2-}	0.005	0.003
I^-	0.207	0.315
Br^-	0.277	0.203
Cl^-	0.267	0.155
CrO_4^{2-}	0.019	0.014

Lifetime evaluation of the ISE

To determine the lifetime of the unmodified and modified graphite-epoxy printed electrodes with PVC matrix membranes, the selection criterion was the time during which the electrode maintains a logarithmic relationship between the potential and log a(NO_3^-) of the Nernst type, a criterion reported by other authors [29,48]. Figure 9 shows the behavior of the slope response of the electrodes as a function of time, determined in triplicate at 2, 11, 30 and 120 days. For both electrodes, a Nernst-type behavior was observed during the time analysed, according to the error margins reported, since they exhibited sensitivity values close to the theoretical value reported by Nernst for a monovalent anion. The study suggests that the electrodes constructed have a lifetime greater than 120 days.

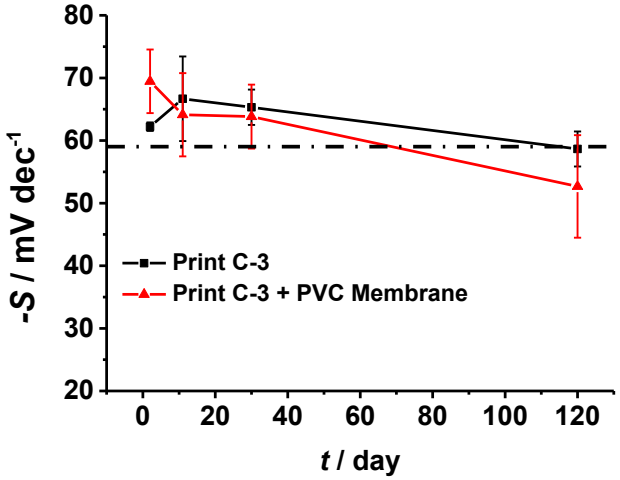

Figure 9. *Sensitivity behavior as a function of time for the unmodified and modified graphite-epoxy printed electrodes with PVC membranes*

An important aspect of the electrodes produced in this research is their reusability for successive measurements and their lifetime. This made it possible to study different parameters of the

electrodes without them losing their response. This feature is an important advantage over commercial printed electrodes, which are designed to be used and discarded.

Application of PVC membrane modified electrodes for indirect potentiometric determination of chloride ions in synthetic water samples

The results discussed above show that the developed printed electrodes selective for nitrate ions have potential for use in environmental analysis. This allowed the development of teaching laboratory practices with the printed electrodes modified with white PVC membranes. The low response of the ISE to other ions, such as Cl^- ions, allowed the indirect potentiometric determination of this ion in synthetic samples by volumetric precipitation with $AgNO_3$. Figure 10 shows the potentiometric titration curves obtained for five electrodes at two levels of chloride ion concentration (0.01 and 0.05 mol L^{-1}, respectively).

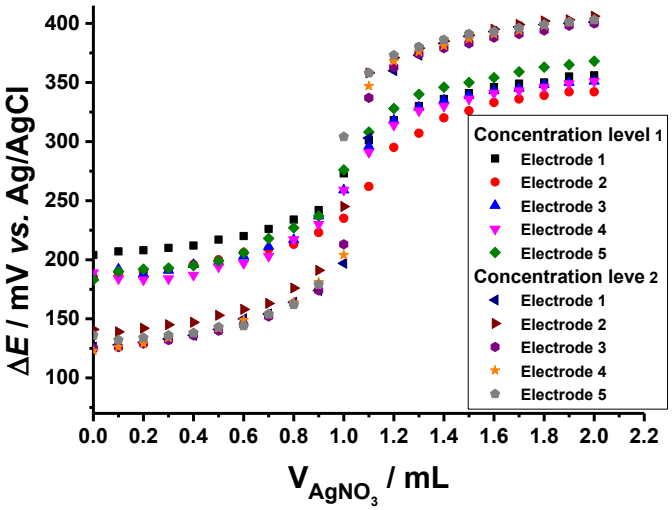

Figure 10. *Potentiometric titration curve for 5 printed electrodes modified with PVC membranes, at two levels of chloride ion concentration. Titrant $AgNO_3$ at 0.01 mol L^{-1} (1st concentration level) and 0.1 mol L^{-1} (2nd concentration level)*

The Nikolsky equation (Equation (2)) explains why it was possible to determine the concentration of chloride ions with nitrate ion-selective electrodes. During the potentiometric titration, the concentration of nitrate ions increases and that of chloride ions decreases linearly until the equivalence point is reached. After this point, the nitrate ions remain in excess, causing a large increase in the potentiometric potential.

$$\Delta E = K - 0.059 \log\left(a_{NO_3^-} + K^{pot}_{NO_3^-,Cl^-} a_{Cl^-}^{Zn_{NO_3^-}/Z_{Cl^-}}\right) \quad (2)$$

The variation of the potential during the titration is mainly due to the value of the potentiometric selectivity coefficient and the concentration of the chloride and nitrate ions. Before the equivalence point, the potential difference of the system is a function of the concentration of the interfering ion (chloride ions), since the product of the activity of this ion and the potentiometric selectivity coefficient is greater than the activity of the nitrate ion, since the concentration of nitrate ions is very low at the beginning of the titration. After the equivalence point, the potential difference of the system is a function of the activity of the nitrate ion (primary ion), since the activity of the interfering ion is less than that of the nitrate ion by the potentiometric selectivity coefficient. Consequently, the potential difference will vary from lower to higher values after the potential jump.

During the classroom practice, each electrode was analysed by two different students and the titration curves were performed in duplicate at two concentration levels to validate the manufactured electrodes. A three-factor nested design (analysis of variance, ANOVA) was performed on the concentration data obtained experimentally, allowing the precision to be estimated under repeatability conditions and under intermediate precision conditions between operators, between electrodes and between operators and electrodes. After confirming the homogeneity of the variances with 95 % confidence, the precision estimates were calculated for each of the concentration levels evaluated, whose values are presented in Table 8.

Table 8. *Estimated precision for each concentration level*

	C_{Cl^-} / mol L^{-1}	
	Level 1	Level 2
	0.01	0.05
	Precision estimation (concentration estimation)	
S_r	0.00048	0.0021
S_A	0.00048	0.0024
S_E	0.00055	0.0032
S_{EA}	0.00056	0.0034

S_r: Estimated accuracy under repeatability conditions
S_A: Estimated accuracy under medium accuracy conditions - operator
S_E: Estimated accuracy under medium accuracy conditions - electrode
S_{EA}: Estimated accuracy under intermediate accuracy conditions - electrode – operator

Accuracy estimates increase from the repeatability level to the intermediate accuracy level under electrode analyser conditions. An increase in imprecision as one moves up the nested design is due to a greater number of factors contributing to the variance in accuracy. The variance between S_r and S_A levels is less than the variance between S_E and S_{EA} levels, indicating that the greatest variability is obtained between electrodes and the contribution of the operator and replicate variables have less influence on the error in concentration estimation. In addition, it is observed that the values of intermediate precision operator, electrode and electrode-operator and precision in repeatability conditions, show adequate values of repeatability and precision of the electrodes in the determination of the concentration of Cl^- ions for teaching laboratory practices. These results strengthen the potential of application in environmental samples.

The comparison of the theoretical concentration values, calculated according to the mass of the weighed salt, and the concentration estimated using the printed electrodes selective for nitrate ions, shows that the electrodes allow the determination of the concentration of Cl^- ions with a low bias, since the relative standard deviation reported values lower than 20 % for both concentration levels (4.01 and 5.77 % respectively)

Conclusions

Epoxy graphite electrodes were printed under repeatability conditions, with a composition of 76 % graphite (7.6 % of nanometer graphite and 68.4% of 50 µm graphite) and a 1:4 volume ratio of 1-butanol: benzyl alcohol. The modification of the carbon inks with nanometric graphite imparted a better electrochemical behavior to the developed electrodes. The variations in the potentiometric responses of the electrodes could be related to the modifications that the surface of the different electrodes undergoes after the activation process. The increase in sensitivity of electrodes activated with lead nitrate (II) could be due to response mechanisms generated by the possible presence of amine salts in the transducer, favoring the exchange of nitrate ions through the membrane phase. The analytical characteristics of the electrodes developed in this work make it a potential proposal

for use in the analysis of nitrate ions in real samples; due to their precision, repeatability, selectivity, wide linear range of response (between 4×10^{-2} and 22 mmol L^{-1}) and low detection limits.

***Acknowledgements**: The research leading to the results presented in this publication was funded by the International Funds and Projects Management Office under the code PN223LH010-055. To the Institute of Materials Science and Technology (IMRE) for the SEM analysis of the electrodes. To the Nanosciences Group of the Center for Technological Applications and Nuclear Development for the synthesis of nanometric graphite.*

***Competing financial interests**: The authors declare no competing financial interest.*

References

[1] J. D. Bolaños-Alfaro, G. Cordero-Castro, G. Segura-Araya, Determinación de nitritos, nitratos, sulfatos y fosfatos en agua potable como indicadores de contaminación ocasionada por el hombre, en dos cantones de Alajuela (Costa Rica), *Revista Tecnología en Marcha* **30** (2017). https://doi.org/10.18845/tm.v30i4.3408 (in Spanish)

[2] P. Mishra, B. Jain, R. D. Shukla, O. Dagdag, E. E. Ebenso, M. K. Tyagi, E. Berdimurodov, D. K. Verma, R. Patel, K. Berdimuradov, A review on the determination methods of nitrate and the routes for its removal from environmental samples, *International Journal of Environmental Analytical Chemistry* **105** (2025) 33-79. https://doi.org/10.1080/03067319.2023.2247990

[3] S. Wangchuk, K. Promsuwan, J. Saichanapan, A. Soleh, K. Saisahas, K. Samoson, A. Numnuam, P. Kanatharana, P. Thavarungkul, W. Limbut, Cuprous oxide-functionalized activated porous carbon-modified screen-printed carbon electrode integrated with a smartphone for portable electrochemical nitrate detection, *Talanta* **287** (2025) 127581. https://doi.org/10.1016/j.talanta.2025.127581

[4] M. L. Flores, F. V. Toldra, Chemistry, safety, and regulatory considerations in the use of nitrite and nitrate from natural origin in meat products - Invited review, *Meat Science* **171** (2021) 108272. https://doi.org/10.1016/j.meatsci.2020.108272

[5] E. Y. Calleros-Rincón, R. P. Morales, A. G. Zamora, J. D. J. Alba-Romero, B. Y. Avalos-Calleros, E. H. Olivas-Calderón, Metahemoglobina y cuerpos de Heinz como biomarcador de exposición a nitratos en niños, *Revista Latinoamericana el Ambiente y las Ciencias* **9(21)** (2018) 15-29. https://rlac.buap.mx/sites/default/files/9%2821%29-2.pdf (in Spanish)

[6] A. K. Nussler, M. Glanemann, A. Schirmeier, L. Liu, N. C. Nüssler, Fluorometric measurement of nitrite/nitrate by 2, 3-diaminonaphthalene, *Nature Protocols* **1** (2006) 2223-2226. https://doi.org/10.1038/nprot.2006.341

[7] D. Tsikas, Analysis of nitrite and nitrate in biological fluids by assays based on the Griess reaction: appraisal of the Griess reaction in the L-arginine/nitric oxide area of research, *Journal of Chromatography B* **851** (2007) 51-70. https://doi.org/10.1016/j.jchromb.2006.07.054

[8] H. Kodamatani, S. Yamazaki, K. Saito, T. Tomiyasu, Y. Komatsu, Selective determination method for measurement of nitrite and nitrate in water samples using high-performance liquid chromatography with post-column photochemical reaction and chemiluminescence detection, *Journal of Chromatography A* **1216** (2009) 3163-3167. https://doi.org/10.1016/j.chroma.2009.01.096

[9] M. O. Mendoza, O. Arias de Fuentes, E. Prokhorov, G. L. Barcenas, E. P. Ortega, Correlation between Electrical Properties and Potentiometric Response of CS‐Clay Nanocomposite Membranes, *Advances in Materials Science Engineering* **2015** (2015) 710425. https://doi.org/10.1155/2015/710425

[10] R. K. Mahajan, R. Kaur, H. Miyake, H. Tsukube, Zn (II) complex-based potentiometric sensors for selective determination of nitrate anion, *Analytica Chimica Acta* **584** (2007) 89-94. https://doi.org/10.1016/j.aca.2006.11.011

[11] M. Schlagmann, J. Balendonck, T. Otto, M. B. Silva de Assis, M. Mertig, S. Hess, Development of sensor nodes and sensors for smart farming, *Journal of Electrochemical Science Engineering* **13** (2023) 825-838. https://doi.org/10.5599/jese.1645

[12] A. Calvo-López, E. Arasa-Puig, M. Puyol, J. M. Casalta, J. Alonso-Chamarro, Biparametric potentiometric analytical microsystem for nitrate and potassium monitoring in water recycling

processes for manned space missions, *Analytica Chimica Acta* **804** (2013) 190-196. https://doi.org/10.1016/j.aca.2013.10.013

[13] L. Zhang, M. Zhang, H. Ren, P. Pu, P. Kong, H. Zhao, Comparative investigation on soil nitrate-nitrogen and available potassium measurement capability by using solid-state and PVC ISE, *Computers and Electronics in Agriculture* **112** (2015) 83-91. https://doi.org/10.1016/j.compag.2014.11.027

[14] M. O. Mendoza, E. P. Ortega, O. Arias de Fuentes, Y. Prokhorov, J. G. Luna-Barcenas, *2014 IEEE 9th IberoAmerican Congress on Sensors*, *Chitosan/bentonite nanocomposite: Preliminary studies of its potentiometric response to nitrate ions in water*, Bogota, Colombia, 2014, pp. 1-4.

[15] A. G. Miranda-Ferrari, S.J . Rowley-Neale, C. E. Banks, Screen-printed electrodes: Transitioning the laboratory in-to-the field, *Talanta Open* **3** (2021) 100032. https://doi.org/10.1016/j.talo.2021.100032

[16] R. Koncki, S. Głąb, J. Dziwulska, I. Palchetti, M. Mascini, Disposable strip potentiometric electrodes with solvent-polymeric ion-selective membranes fabricated using screen-printing technology, *Analytica Chimica Acta* **385** (1999) 451-459. https://doi.org/10.1016/S0003-2670(98)00726-0

[17] H. Jiang, W. Yu, J.F. Waimin, N. Glassmaker, N. Raghunathan, X. Jiang, B. Ziaie, R. Rahimi, *2019 IEEE SENSORS*, *Inkjet-printed solid-state potentiometric nitrate ion selective electrodes for agricultural application*, Montreal, QC, Canada, 2019, pp. 1-4.

[18] C.L. Baumbauer, P.J. Goodrich, M.E. Payne, T. Anthony, C. Beckstoffer, A. Toor, W. Silver, A.C. Arias, Printed Potentiometric Nitrate Sensors for Use in Soil, *Sensors* **22** (2022) 4095. https://doi.org/10.3390/s22114095

[19] N. Thi DieuThuy, X. Wang, G. Zhao, T. Liang, Z. Zou, A Co_3O_4 Nanoparticle-Modified Screen-Printed Electrode Sensor for the Detection of Nitrate Ions in Aquaponic Systems, *Sensors* **22** (2022) 9730. https://doi.org//10.3390/s22249730

[20] F. Paré, A. Visús, G. Gabriel, M. Baeza, Novel Nitrate Ion-Selective Microsensor Fabricated by Means of Direct Ink Writing, *Chemosensors* **11** (2023) 174. https://doi.org/10.3390/chemosensors11030174

[21] L. C. Fajardo, A. I. Balbin-Tamayo, A. M. Esteva-Guas, Characterization of graphite-epoxy composite electrodes for free electrochemical detection of adenine and guanine in DNA, *Journal of Electrochemical Science Engineering* **11** (2021) 247-261. https://doi.org/10.5599/jese.1005

[22] L. H. Tabares, J. G. Darias-González, J. A. Díaz, E. C. Barroso, L. M. Ledo-Pereda, L. F. Desdín-García, Automated system for the synthesis of nanostructures via arc-discharge in liquids, *Advances in Natural Sciences: Nanoscience Nanotechnology* **9** (2018) 035002. https://doi.org/10.1088/2043-6254/aad1a6

[23] L. Hernandez-Tabares, S. Fortune-Fabregas, F. J. Chao-Mujica, J. G. Darias-Gonzalez, N. Torres-Figueredo, E. Reguera, L. F. Desdin-Garcia, Multiparametric diagnostic in the synthesis of carbon nanostructures via submerged arc discharge: Stability, nucleation and yield, *Journal of Applied Physics* **126** (2019). https://doi.org/10.1063/1.5108815

[24] L. H. Tabares, J. G. Darias-Gonzalez, F. J. Chao-Mujica, L. M. Ledo-Pereda, M. Antuch, E. C. Barroso, J. E. Chong-Quero, E. Reguera, L. F. Desdin-Garcia, Stabilization methods in the submerged arc discharge synthesis of carbon nanostructures, *Journal of Nanomaterials* **2021** (2021) 6550809. https://doi.org/10.1155/2021/6550809

[25] L. F. Desdín-García, F. J. Chao-Mujica, L. H. Tabares, L. G. Hernández, J. G. Darias-González, L. M. Ledo-Pereda, Á. L. Corcho-Valdés, M. A. Cubillas, Progress in the synthesis of carbon nanostructures by submerged arc discharge, *Nucleus (Havana)* **73** (2023) 25-28. http://nucleus.cubaenergia.cu/index.php/nucleus/article/view/783/1124 (in Spanish)

[26] M. d. l. A. Arada-Pérez, M. Y. Pedram, J. Marín, A.S . Planche, Estudio del reconocimiento molecular de un portador movil neutro usado como electrodo all solid state a nitrato, *Afinidad* **66** (2009) 134-138. https://raco.cat/index.php/afinidad/article/view/276777/364704 (in Spanish)

[27] A. R. Lazo-Fraga, M. B. Bustamante, M. Arada, J. Jiménez, M. Yazdani-Pedram, Construction and characterization of a lead(II) ion selective electrode with 1-furoil-3,3-diethylthiourea as neutral carrier, *Afinidad -Barcelona* **62** (2005) 606-610. https://www.researchgate.net/publication/40883201_Construction_and_characterization_of_a_lead_II_ion_selective_electrode_with_1-furoil-33-diethylthiourea_as_neutral_carrier

[28] A. I. Balbín-Tamayo, L. S. Riso, A. P. Gramatges, P. A. Marini-Farías, A. M. Esteva-Guas, Electro-chemical characterization a new epoxy graphite composite electrode as transducer for biosensor, *Sensors Transducers* **202** (2016) 59-65. https://www.sensorsportal.com/HTML/DIGEST/july_2016/Vol_202/P_2841.pdf

[29] M. G. Quintela, M. V. Portales, A. M. Díaz-García, M. B. Sánchez, G. S. Díaz, A. R. Lazo-Fraga, O. E. Hernández, On the analytical response of lead (II) selective electrodes using 1-aroyl-3, 3-dimethylthioureas as ionophores: membrane analysis and quantum chemical calculations, *Phosphorus, Sulfur, Silicon the Related Elements* **197** (2022) 1213-1225. https://doi.org/10.1080/10426507.2022.2085270
[30] Statgraphics Centurion 19, https://www.statgraphics.com/centurion-overview (March 3, 2025).
[31] R.P. Buck, L. Erno, Recommendations for nomenclature of ionselective electrodes (IUPAC Recommendations 1994), *Pure and Applied Chemistry* **66** (1994) 2527-2536. https://doi.org/10.1351/pac199466122527
[32] C. Maccà, Response time of ion-selective electrodes: Current usage versus IUPAC recommendations, *Analytica Chimica Acta* **512** (2004) 183-190. https://doi.org/10.1016/j.aca.2004.03.010
[33] J. M. Pingarrón-Carrazón, P. S. Batanero, *Química Electroanalítica, Fundamentos y Aplicaciones*, Editorial Síntesis S.A., Madrid, España, 2003, p. 148-151. ISBN 978-8477386636 (in Spanish)
[34] R. S. Nicholson, Theory and Application of Cyclic Voltammetry for Measurement of Electrode Reaction Kinetics, *Analytical Chemistry* **37** (1965) 1351-1355. https://doi.org/10.1021/ac60230a016
[35] L. Matějka, J. Lövy, S. Pokorný, K. Bouchal, K. Dušek, Curing epoxy resins with anhydrides. Model reactions and reaction mechanism, *Journal of Polymer Science: Polymer Chemistry Edition* **21** (1983) 2873-2885. https://doi.org/10.1002/pol.1983.170211003
[36] M. d. l. A. Arada-Pérez, Y. M. P. Pedram-Zobeiri, Chemical sensor based on tetradecil ammonium nitrate, *Journal of the Chilean Chemical Society* **58** (2013) 1545-1548. https://doi.org/10.4067/S0717-97072013000100010
[37] M. d. l. A. Arada-Pérez, K. Y. Nápoles-Florián, J. M. Rodríguez-Acebal, M. Y. Pedram, A. R. Lazo-Fraga, Nitrate determination in natural water samples by potentiometry with ion selective electrode, *Revista Cubana de Química* **34** (2022) 242-262. https://cubanaquimica.uo.edu.cu/index.php/cq/article/view/5241
[38] S. Amemiya, P. Bühlmann, K. Odashima, A generalized model for apparently "non-nernstian" equilibrium responses of ionophore-based ion-selective electrodes. 1. Independent complexation of the ionophore with primary and secondary ions, *Analytical Chemistry* **75** (2003) 3329-3339. https://doi.org/10.1021/ac026471g
[39] S. Amemiya, *Potentiometric ion-selective electrodes*, Elsevier, 2007, p. 261-294 https://doi.org/10.1016/B978-044451958-0.50020-3.
[40] S. Moulay, Chemical modification of poly (vinyl chloride)—Still on the run, *Progress in Polymer Science* **35** (2010) 303-331. https://doi.org/10.1016/j.progpolymsci.2009.12.001
[41] W. G. Vasquez, L. Dammak, C. Larchet, V. Nikonenko, D. Grande, Effects of acid–base cleaning procedure on structure and properties of anion-exchange membranes used in electrodialysis, *Journal of Membrane Science* **507** (2016) 12-23. https://doi.org/10.1016/j.memsci.2016.02.006
[42] R. Bacaloglu, M. Fisch, Degradation and stabilization of poly (vinyl chloride). V. Reaction mechanism of poly (vinyl chloride) degradation, *Polymer Degradation and Stability* **47** (1995) 33-57. https://doi.org/10.1016/0141-3910(94)00086-N
[43] E. M. Bomar, G. S. Owens, G. M. Murray, Nitrate ion selective electrode based on ion imprinted poly (N-methylpyrrole), *Chemosensors* **5** (2017) 2. https://doi.org/10.3390/chemosensors5010002
[44] S. S. M. Hassan, A. G. Eldin, A. E. G. E-Amr, M. A. Al-Omar, A. H. Kamel, N. M. Khalifa, Improved solid-contact nitrate ion selective electrodes based on multi-walled carbon nanotubes (MWCNTs) as an ion-to-electron transducer, *Sensors* **19** (2019) 3891. https://doi.org/10.3390/s19183891
[45] Oficina Nacional de Normalización (NC), www.nc.cubaindustria.cu (in Spanish), (May 23, 2018).
[46] SCRIBD, https://es.scribd.com/docs (June 8, 2025).
[47] E. Bakker, P. Bühlmann, E. Pretsch, Carrier-based ion-selective electrodes and bulk optodes. 1. General characteristics, *Chemical Reviews* **97** (1997) 3083-3132. https://doi.org/10.1021/cr940394a
[48] L. Zhang, Z. Wei, P. Liu, An all-solid-state NO_3-ion-selective electrode with gold nanoparticles solid contact layer and molecularly imprinted polymer membrane, *PLoS One* **15** (2020) e0240173. https://doi.org/10.1371/journal.pone.0240173